ELSEVIER

Solid State Ionics 131 (2000) 199–210

SOLID STATE IONICS

www.elsevier.com/locate/ssi

A novel technique for imaging electrochemical reaction sites on a solid oxide electrolyte

T. Kawada[a,*], T. Horita[b], N. Sakai[b], H. Yokokawa[b], M. Dokiya[c], J. Mizusaki[a]

[a]*Research Institute for Scientific Measurements, Tohoku University 2-1-1, Katahira, Aoba-ku, Sendai 980-8577 Japan*
[b]*National Institute of Materials and Chemical Research, Tsukuba Research Center, Ibaraki 305, Japan*
[c]*Institute of Environmental Science and Technology, Yokohama National University, Tokiwadai, Hodogaya-ku, Yokohama 240, Japan*

Received 11 August 1998; received in revised form 29 October 1998; accepted 5 November 1998

Abstract

Oxygen isotope was used to investigate the active electrochemical reaction site on a solid oxide electrolyte. The isotope exchange reaction was performed under current flow, and the distribution of the incorporated isotope was analyzed by a secondary ion mass spectrometer. The results were compared with calculations using a simple model. The lateral resolution of the present method was estimated to be around 1 μm. The quenching process and the imaging resolution should be improved to investigate further details. © 2000 Elsevier Science B.V. All rights reserved.

Keywords: Electrochemical reaction site; $^{18}O/^{16}O$; Isotope exchange; SIMS

Materials: Platinum; Yttria stabilized zirconia; Oxygen

1. Introduction

Kinetics of electrochemical reactions on a solid oxide electrolyte have been widely investigated by many researchers not only from scientific interest but also from technological requirements. The improvement of the electrodes can often be a key technology in a practical application such as gas sensors, solid oxide fuel cells, or oxygen separation membranes. Although much effort has been made to understand the electrode reaction process, there still remain many unsolved problems. Among them, one of the most essential question is "where in the electrode does the electrochemical reaction take place?". In a gas/porous electrode/oxide electrolyte system, the most preferable electrochemical reaction site is undoubtedly a triple phase boundary (TPB) of electrode/electrolyte/gas, where electron, oxide ion and the gaseous species meet together [1]. In some cases, however, the active reaction area extends to the electrode surface, to the free electrolyte surface or to the electrode/electrolyte two phase boundaries. Since the extension of the reaction site is related to the kinetic parameters, misunderstanding will lead to a wrong interpretation of the experimental data as pointed out by several authors [2–4]. The knowledge of the active reaction site is thus essential for the basic kinetic analysis of the experimental data.

*Corresponding author. Tel.: +81-22-217-5341; fax: +81-22-217-5343.

E-mail address: kawada@rism.tohoku.ac.jp (T. Kawada)

0167-2738/00/$ – see front matter
PII: S0167-2738(00)00634-2

Similarly, in designing a practical electrode, knowledge on both microscopic and macroscopic current distribution is necessary. The microscopic distribution is related to the reaction kinetics as mentioned above and is important for the design of the electrode material and microstructure. The macroscopic current distribution is important in improvement of current collection. The both will seriously affect the electrode performance.

Regardless of the importance, an experimental technique has never been developed for getting direct information on the electrode reaction site. So far, the research works have been performed only with indirect experiments, e.g. measurement of I–V curve or ac impedance responses as a function of the electrode morphology. One of the ideas to get direct information on the reaction site is to observe the trace of the oxide ion migration in the electrolyte. This may be possible by using an oxygen isotope, $^{18}O_2$, and secondary ion mass spectrometer (SIMS) with imaging capability. The similar technique has been successfully applied in the investigation of diffusion coefficients or fast diffusion paths in ceramics [5–7] or preferable oxidation sites in metals.

The authors have been trying to develop an experimental technique to visualize the active reaction site on a solid oxide electrolyte with a porous platinum electrode [8] and with a patterned $(La,Sr)MNO_3$ electrode [9]. In this paper, the experimental procedure for the isotope imaging is reported in detail. A numerical calculation is performed to evaluate the preferable experimental condition for the active site imaging. The experimental result with a porous Pt electrode will be compared with the calculation. The merit and the limitation of this method will be discussed.

2. The method for imaging the active site

2.1. Experimental procedure

Fig. 1 outlines the experimental procedure for determining the active reaction site on a solid oxide electrolyte. The sample is first equilibrated in a certain atmosphere, and then exposed to ^{18}O enriched gas of the same oxygen potential. After a period the sample is quenched and the isotope distribution is measured by SIMS. This sequence is quite similar to that used for determining oxygen isotope diffusion coefficient [7]. The only difference is that the sample has electrodes and oxide ionic current is flowing during the equilibration and the isotope exchange processes. If the cathodic current is applied to the electrode, the isotope enriched oxygen will be incorporated from the active electrochemical reaction site, and the resulting isotope distribution in the quenched sample will give information on the

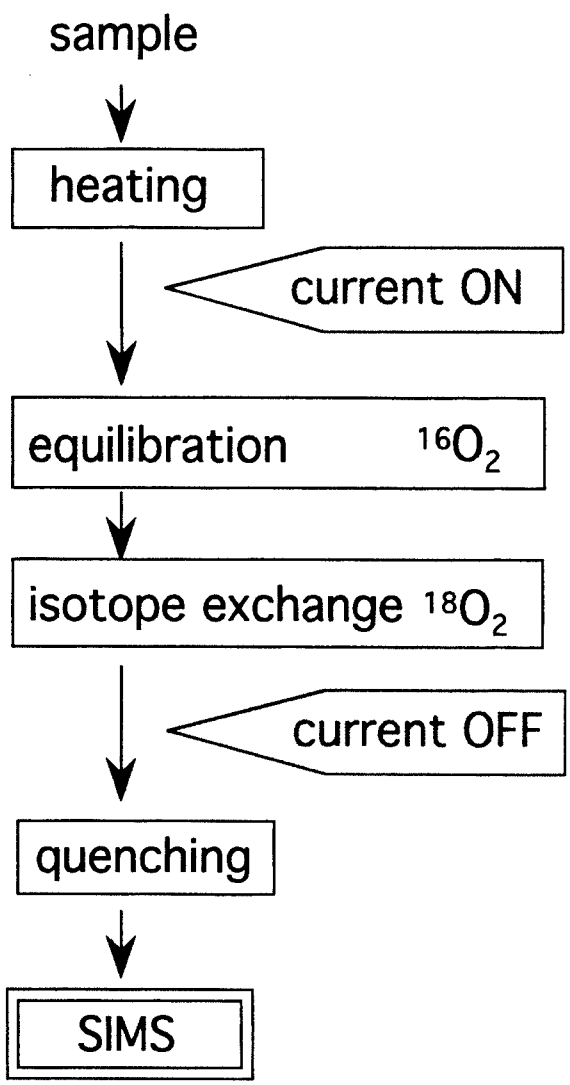

Fig. 1. Schematic diagram of the experimental procedure for imaging electrochemical active sites on a solid oxide electrolyte.

active reaction site. In principle, the anodic reaction can also be imaged by comparing the isotope profiles with and without electrical current. For such an analysis, however, a well defined electrode and highly reproducible experiments are required, which are technologically difficult in our present equipment. In this report, only cathodic reaction is considered.

2.2. Required conditions

The isotope mapping of the active reaction site is not always possible. This is because the isotope exchange reaction takes place not only by the electrochemical oxygen incorporation at the active site but also by the exchange of neutral oxygen on the free electrolyte surface. If the surface exchange process is too fast, the isotope concentration becomes high at the surface and will hide the trace of the electrochemically incorporated isotope. The surface isotope concentration is determined by the ratio of the surface reaction rate k^* and the isotope diffusion coefficient D^*. When k^* is much larger than D^*, the isotope concentration on the sample surface is close to that in the gas phase. In such a case, the electrochemical incorporation of the isotope is not detectable. The atmosphere, temperature and annealing time in the experiment must be chosen to accomplish that k^* is sufficiently smaller than D^*. The other requirement is fast quenching. Otherwise, the isotope distribution pattern will diffuse away in the quenching procedure. In case of YSZ electrolyte, oxygen isotope diffuses several microns if it is kept for 10 s at 1000 K. Thus, the sample temperature must decrease below 1000 K in less than a second to get the imaging resolution higher than 1 μm.

2.3. Numerical calculation

Numerical calculations were performed to predict the isotope distribution pattern around the active reaction site. The differential equation of Fick's second law was solved using a finite element method ('MARC K-6', Nippon Marc Co.). A simple model of a stripe shaped electrode was defined as shown in Fig. 2. For simplicity, the following boundary conditions were used:

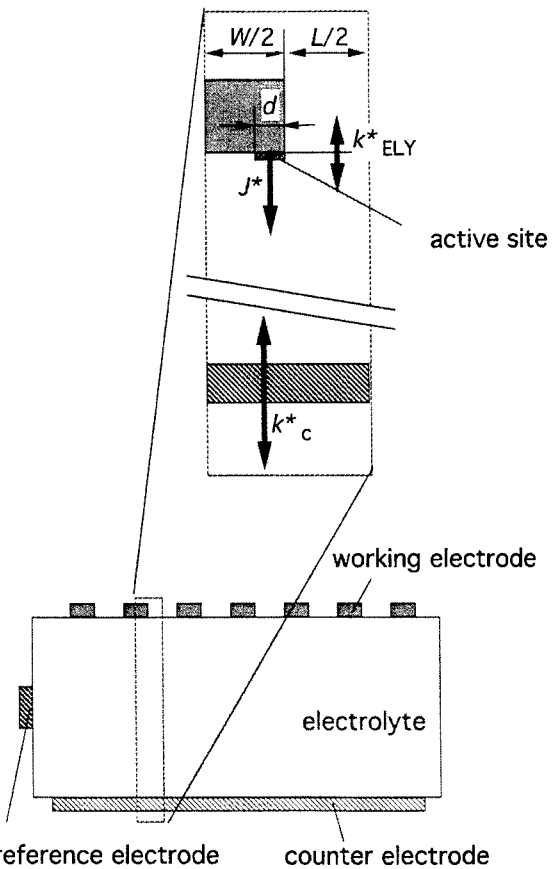

Fig. 2. A two dimensional electrode model to simulate the isotope distribution pattern. The working electrode is stripe shaped. The calculation was done for the unit cycle surrounded by the square in the figure. The parameters used for the calculation are listed in Table 1.

1. The isotope flux is zero on the electrode/electrolyte two phase boundary except for the electrochemical reaction site.
2. The active electrochemical reaction site has a limited width around the TPB, and the oxide ion (isotope) flux is homogeneous inside this area.
3. Only isotope diffusion is considered inside the electrolyte. Migration of the oxide ion under the electrical field is neglected. The effect of the electrical current is included in the calculation as the increase of isotope incorporation flux at the active reaction site.
4. The ionic flux density at the reaction site was estimated by dividing the apparent current density by the total TPB length in unit area.

5. The oxygen isotope diffusion coefficient in the electrolyte and the surface exchange coefficient on the free electrolyte surface were estimated from a separate isotope diffusion experiment.
6. The surface exchange rate at the counter electrode was assumed to be infinity.

The parameters used in the calculation are listed in Table 1.

Fig. 3 shows the calculated isotope concentration

Table 1
The parameters used in the calculation of isotope distribution

Electrode pattern width	W	5 μm
Electrode pattern distance	L	5 μm
Active reaction site width	d	0.0625 to 1 μm
Temperature	T	973 K
Isotope diffusion coefficient	D^*	5.7×10^{-8} cm^2 s^{-1}
Surface exchange coefficient	k^*	3.0×10^{-8} cm s^{-1}
Apparent current density	J	0.15–15 mA cm^{-2}

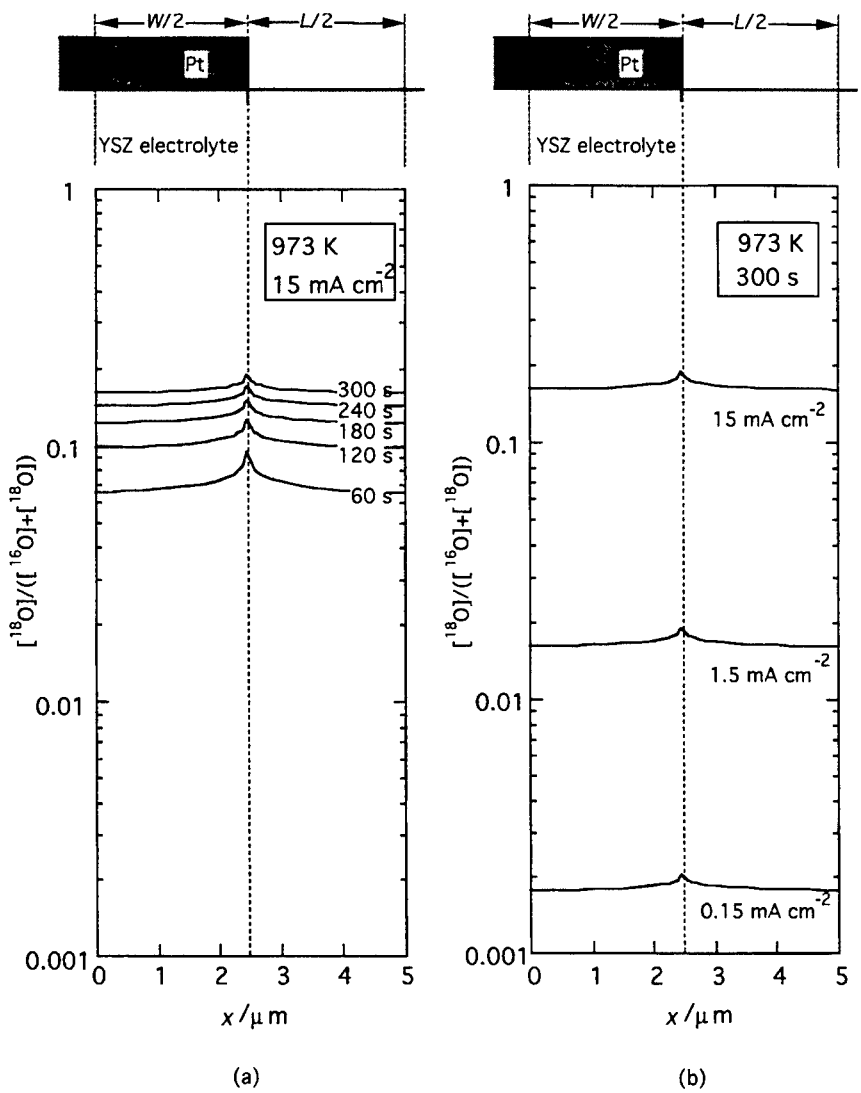

Fig. 3. Dependence of the calculated isotope concentration profile on reaction time (a) and ionic current density (b). The parameters in the standard condition are listed in Table 1.

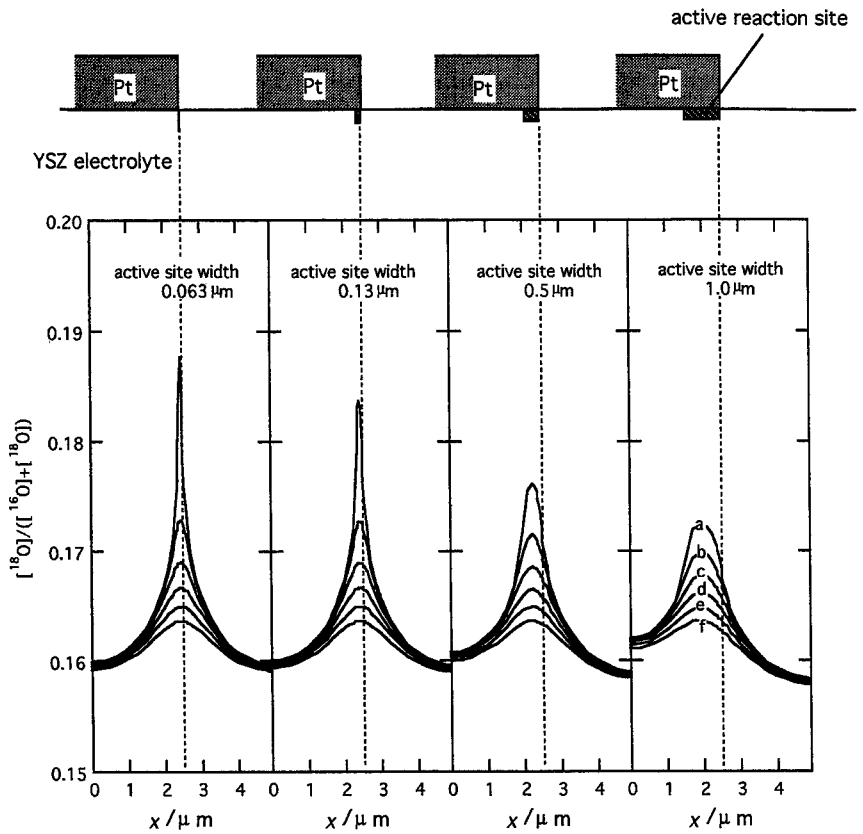

Fig. 4. Dependence of calculated isotope distribution on the active site width. The curves are isotope concentration profile in the depth of the electrolyte (a) 0 μm (b) 0.031 μm, (c) 0.063 μm, (d) 0.09375 μm, (e) 0.125 μm and (f) 0.15625 μm.

profile at the surface of the electrolyte as functions of (a) the reaction time and (b) the ionic current density. The active reaction site is assumed to extend 0.063 μm from TPB into the electrode/electrolyte two phase boundary. Since the diffusion coefficient is high, the incorporated isotope diffuses quickly into the whole surface of the electrolyte. In the vicinity of TPB, however, the peak of the isotope concentration remains distinguishable from the other parts. If the peak is detected by the SIMS analysis, the information on the reaction site will be obtained. For getting a clearer contrast, shorter reaction time and larger current density are preferred in principle but with small difference.

Fig. 4 compares the calculated profiles with different active site width. The curves in each graph represent the equi-depth isotope concentration profile in the electrolyte which corresponds to the experimental data obtained by successive sputtering and line scanning with SIMS. The high isotope concentration site is observed in the vicinity of the TPB at the surface. The intensity of the isotope fades rapidly with depth in the electrolyte. The peak of the isotope concentration is higher and sharper when the active reaction site is narrower. The resolution of the measurement depends on the lateral resolution of the SIMS equipment. It depends also on the quenching rate which must be fast enough to keep the original distribution of the isotope.

3. Experimental details

3.1. Sample preparation

Commercially available YSZ powder (Y_2O_3 8

mol% doped ZrO_2: TOSOH TZ8Y) was used for preparation of the electrolyte. The powder was pressed into a pellet and sintered at 1780 K for 5 h. The relative density was higher than 99%. The pellet was cut into 5 mm×5 mm×0.3 mm, and the surfaces were polished with diamond paste down to 1/4 micron.

Two platinum electrodes were applied to both surfaces of the sample with an area of 3 mm×3 mm as a working and a counter electrodes. A reference electrode of a smaller size was applied at the periphery of the sample. Each electrode was applied by painting an appropriate amount of platinum paste (Tanaka, TR7905). After heating at 1400 K for 5 h, grain growth of platinum occurred keeping the two dimensional network. The optical photograph of the surface of the sample is shown in Fig. 5. The platinum grains and the bare surface of the YSZ are both visible from the surface. The line between those two parts corresponds to the TPB.

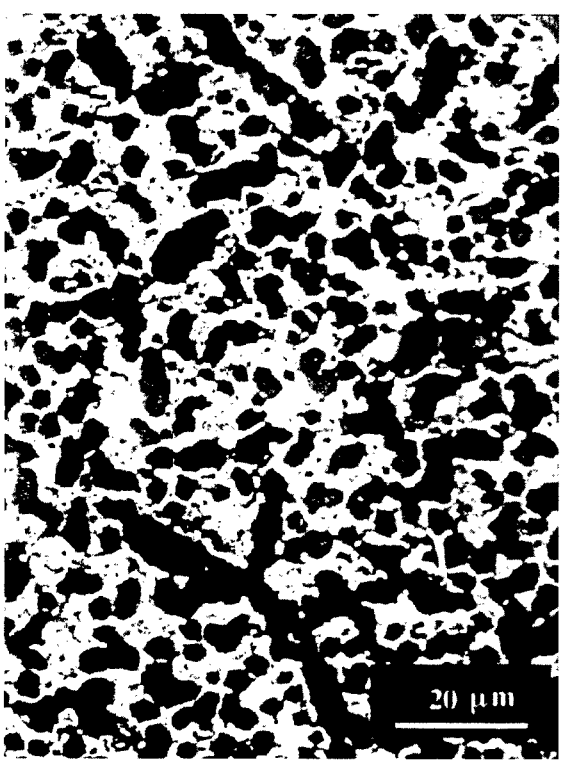

Fig. 5. Optical photograph of the Pt/YSZ surface. Brighter parts are the platinum electrode particles.

3.2. Isotope exchange

Fig. 6 shows the isotope exchange apparatus. The gas circulation chamber consisted of two parts. The left hand side in Fig. 6 is the circulation loop for normal oxygen (natural isotope abundance), and the right hand side is for $^{18}O_2$ enriched (97%) gas. The oxygen pressure in the both loops are adjusted to be same by using a pressure gauge. The sample chamber was connected to the circulation loops via a six-way valve which can choose one of the gases to flow over the sample. As is shown in Fig. 7, three lead wires and a thermocouple were connected to the electrical apparatus through the top part of the cell. Separable connectors ('Quick connects', Swagelock Co.) were used so that the sample chamber was able to be disconnected after isotope exchange operation. An infra-red furnace was used for heating the sample. Gas flowed from the inner tube through the outer tube.

At first, the sample was exposed to the normal oxygen gas and was heated up to a certain temperature (773–1173 K). A potentiostat (TOHO GIKEN 2020) was used to supply current to the sample keeping a constant voltage between the working and the reference electrodes. After a steady state current was reached, the gas was changed abruptly to the $^{18}O_2$ enriched one by the six-way valve. After annealing in $^{18}O_2$, the sample chamber was disconnected from the gas circulation chamber. At the same time, the sample was brought out of the focus of the infra-red furnace, and immediately cooled by blowing cooling gas against the wall of the sample tube. The sample was cooled from 1000 K to 700 K in less than 5 s, and to room temperature in 15 s.

3.3. SIMS analysis

Measurements of the isotope ratio were carried out with a CAMECA ims-5f SIMS equipment. A cesium primary ion beam (Cs^+) was bombarded on the sample at 14.5 keV. The negative secondary ion beam was accelerated at −4.5 keV and analyzed in the mass spectrometer with electronic and magnetic

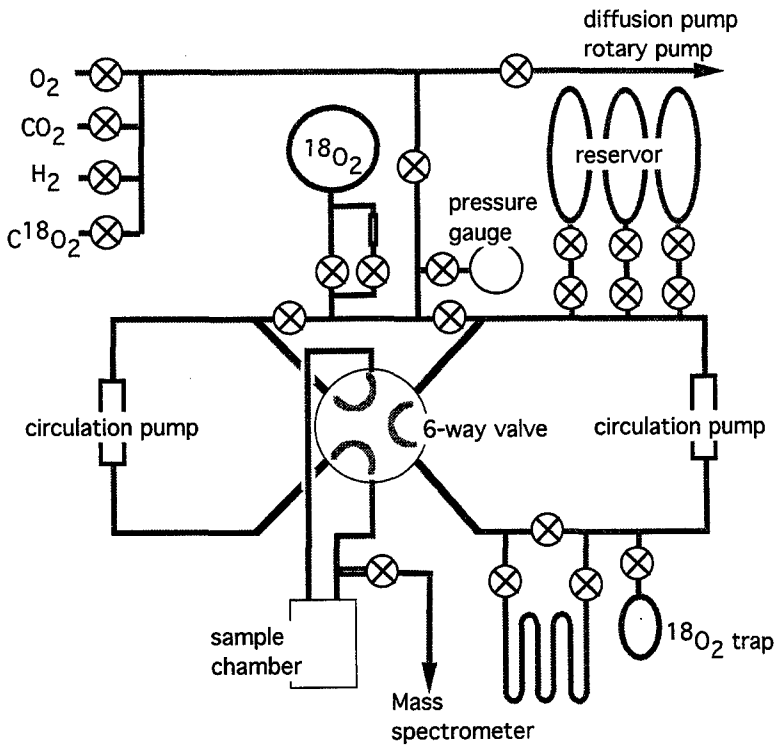

Fig. 6. Schematic view of the isotope exchange equipment (gas circulation system).

sectors. The mass resolution $M/\Delta M$ was about 300 in a normal operation mode, and higher than 7000 in a 'high resolution' operation mode. To distinguish $^{18}O^-$ from $H_2^{16}O^-$, high mass resolution measurements were performed. In all the cases, the signal of $H_2^{16}O^-$ was found to be much smaller than that of $^{18}O^-$. Thus, the imaging experiments were performed in the normal resolution. Since YSZ is an insulator at low temperature, a gold mesh of 250 μm pitch was placed on the sample, and an electron gun was used to compensate for the electric charge.

Two different imaging methods ('microscope' mode and 'micro-probe' mode) were applied to observe the distribution of a selected mass on the sample surface. In the microscope mode, the secondary ion image was focused on a channel plate and observed directly on the screen. The digital image was acquired with a position sensitive detector. The lateral resolution in this mode was about 1 to 2 μm. For a higher resolution image, the micro-probe mode was used, in which the primary beam was focused and scanned on the sample. The lateral resolution depends on the size of the focused primary ion beam, which was around 0.2 μm in our equipment.

4. Results and discussion

4.1. Polarization behavior at 973 K

Fig. 8 shows a steady state polarization curve at 973 K in 0.2 bar oxygen. It showed a characteristic behavior of a Pt electrode on a YSZ electrolyte as reported by Mizusaki et al. [2]. The isotope exchange experiment was performed at the polarization voltage of −0.5 V vs. the reference electrode. The apparent current density over the total electrode area was about -1.5 mA cm^{-2}. After keeping the voltage for 1 h, the $^{18}O_2$ enriched gas was introduced by the six-way valve. The change in the current density was

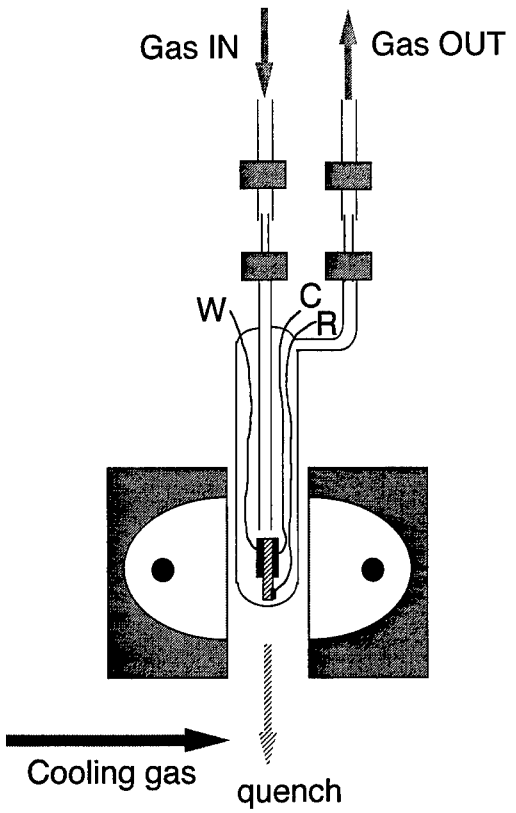

Fig. 7. Sample chamber for the isotope exchange with applying current. The lead wires W, C, R are connected to the working, the counter, and the reference electrodes, respectively.

less than 5% before and after the isotope exchange. The sample was kept for 5 min in $^{18}O_2$, and then, quenched and transferred to SIMS analysis.

4.2. Isotope distribution mapping

Fig. 9(a) shows the $^{16}O^-$ and $^{18}O^-$ secondary ion distribution at the surface of the sample measured by SIMS in the 'microprobe' mode. The brighter spot in the figure represents the higher secondary ion signal. The dark parts correspond to the platinum particles which cover the oxide electrolyte surface. What should be noted in Fig. 9(a) is that the signal of $^{16}O^-$ came homogeneously from the electrolyte part, whereas that of $^{18}O^-$ was localized along the edge of the electrolyte area, i.e. on the triple phase boundaries (TPB).

In Fig. 9(a), not all of the TPB lines were visible

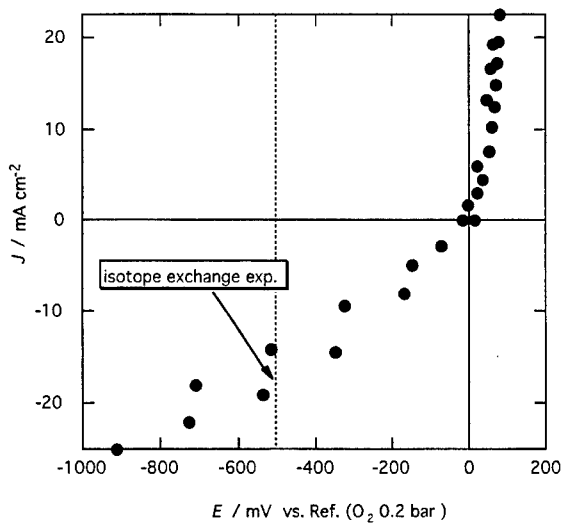

Fig. 8. Steady state polarization curve for Pt/YSZ sample at 973 K in 0.2 bar oxygen.

because some are behind the platinum particles and could not be hit by the primary ion beam of which the incident angle was 30° to the normal. In order to observe the whole TPB lines, the platinum particles were removed by sputtering with a larger primary ion beam (1×10^{-8}A). After 2 min of sputtering, the primary beam current was reduced ($<1\times10^{-10}$ A) and focused again, and the image was acquired. The sputtering and data acquisition cycle was repeated several times. Fig. 9(b)–(d) show the sequential images of the isotope distribution aligned in the order of the sputtering time. By removing the platinum electrode, all of the TPB lines appeared gradually. In the $^{18}O^-$ image, the high intensity sites in the first figure disappeared with sputtering, and new high intensity sites came out around the sputtered edges of the Pt particles. They disappeared by further sputtering. This means that the active reaction site is actually localized around TPB lines.

For quantitative representation, the data in Fig. 9 were scanned on the line A–B, and plotted in terms of total oxygen intensity and the isotope ratio in Fig. 10. Several peaks were observed in the isotope ratio plot. Among them, some peaks were located where the total oxygen intensity is small; i.e. on the platinum particles. Those peaks disappeared much faster than the others by sputtering. They probably came from any contamination on the Pt electrode.

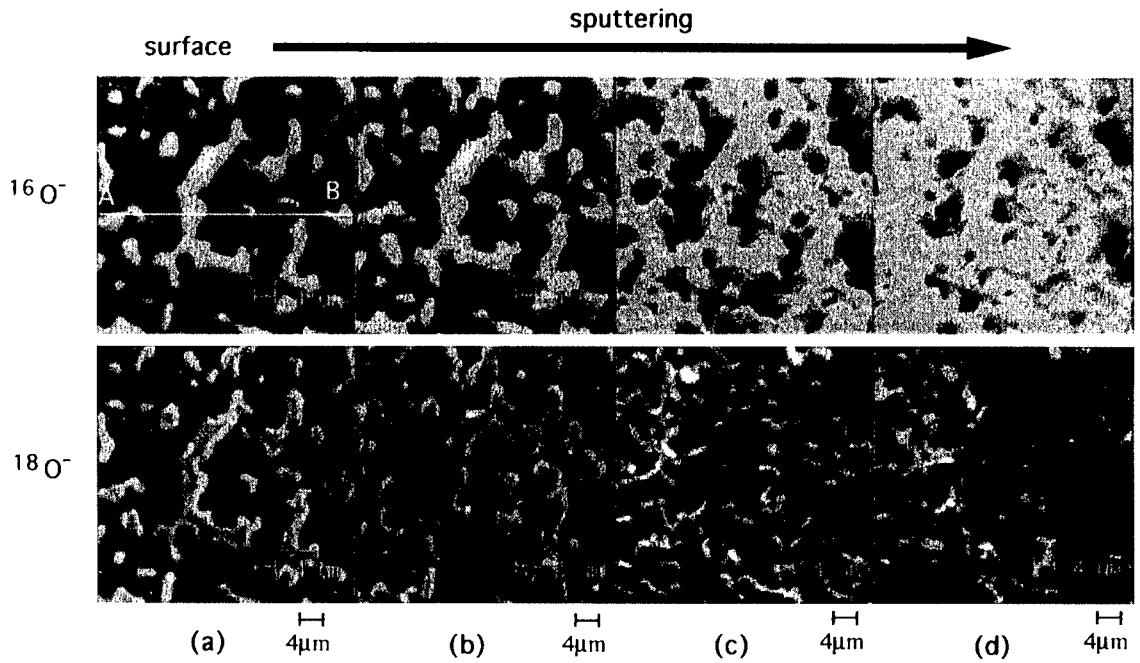

Fig. 9. ^{16}O and ^{18}O distribution in the sample treated at 973 K in 0.2 bar oxygen ^{18}O under cathodic polarization (−0.5 V) for 5 min. Images were taken at the surface (a); after sputtering 2 min. (b); 4 min. (c); and 6 min. (d).

The other peaks were all located around the TPB lines. They are the trace of the electrochemical oxygen incorporation.

The observed isotope profile can be compared with those of the model calculation shown in Fig. 4. The isotope concentration at the surface was around 0.2 at the peaks and 0.05 to 0.1 at the valleys. Most of the peaks disappeared at the last sputtering cycle. Though the exact depth of one sputtering cycle was not clear, it is roughly estimated to be 10–100 nm. From those data, the active reaction site width is estimated to be less than 1 μm. However, the detail of the observed profile is different from the calculation. The further discussion is difficult in the present experiment. In order to determine the reaction site extension in more detail, the electrode of a well defined morphology should be tested, and the quenching speed and the lateral imaging resolution must be improved. Also, the calculation may have to include the effect of oxide ion migration under the electrical field. Due to those limitations, the resolution of the active site imaging in the present experiment may be around 1 μm.

4.3. Reaction site expansion at lower temperature (773 K)

Fig. 11 shows the $^{16}O^-$ and $^{18}O^-$ images of the sample treated under current flow at 773 K. The images were taken in the microscope mode. Unlike the results at 973 K, the $^{18}O^-$ isotope did not distribute along every TPB line. Some 'hot spots' were observed for the isotope incorporation reaction. The existence of the hot spot is an important problem in a practical application. The hot spot generation can be initiated by the existence of any inhomogeneity in morphology of the electrode particles. Current and mass flow may favor extraordinary points such as a valley or a bay of the electrode particles. The existence of any impurity or defect may cause the inhomogeneity of the reaction rate as well. When a hot spot of the reaction is generated, the temperature will increase around those sites and the reaction site becomes further inhomogeneous.

On those hot spots, the active reaction site extended under the platinum electrode particles. When the sputtering process proceeds, the high intensity parts

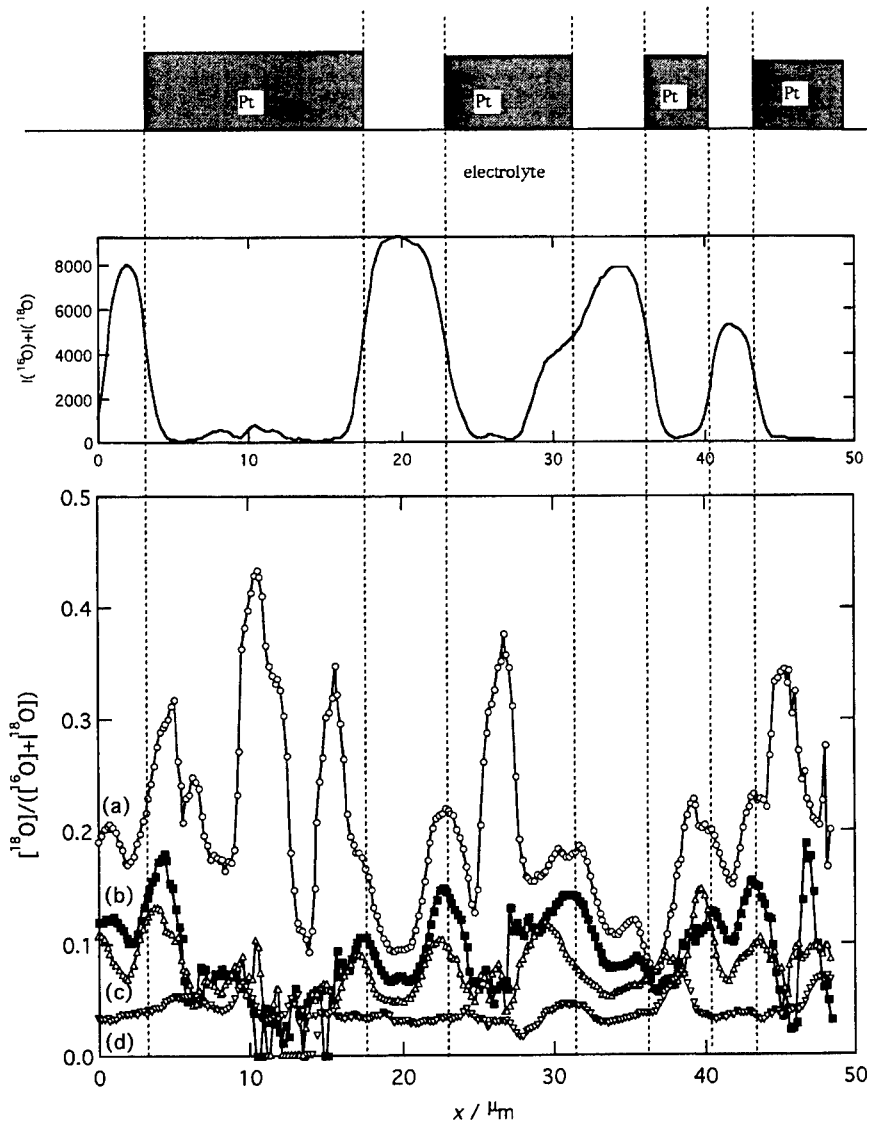

Fig. 10. Total oxygen and isotope concentration profile on the line A–B in Fig. 9. The total oxygen profile is the sum of the ^{16}O and ^{18}O signals in Fig. 9(a).

in $^{18}O^-$ image appeared under the platinum electrode. For example, the two bright spots in Fig. 11(a) became connected after sputtering Pt electrode. The isotope distribution in Fig. 11(d) is rather broad under platinum electrode particles, which suggested that the extension of the active reaction site was large into the platinum/electrolyte two phase boundaries in this experimental condition. The extension can be estimated to be several microns.

4.4. Measurements with the sample treated at higher temperature (1173 K)

Though the same experiments were attempted at 1173 K, no contrast was observed in the isotope distribution. It is probably because the diffusion rate was too large, and the difference of the surface reaction rate was not kept in the profile during the quenching process. Shorter annealing time and faster

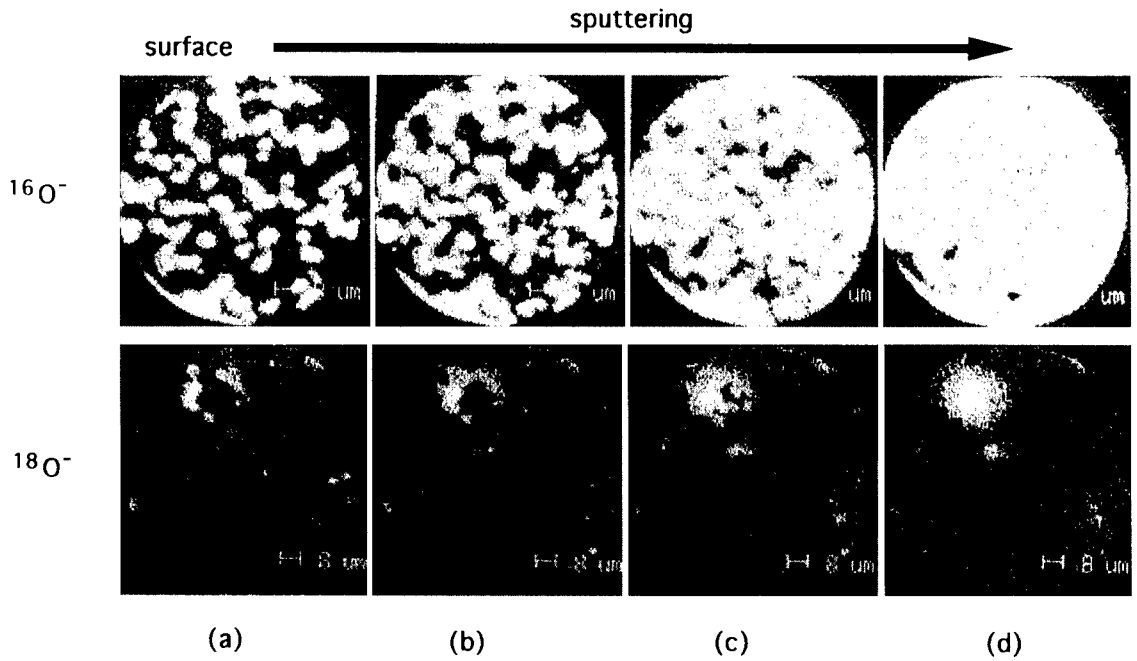

Fig. 11. ^{16}O and ^{18}O distribution in the sample treated at 773 K in 0.2 bar oxygen ^{18}O under cathodic polarization (−0.5 V) for 5 min. Images were taken at the surface (a); after sputtering 2 min. (b); 4 min. (c); and 6 min. (d).

quenching will be necessary for the isotope imaging at higher temperature.

5. Conclusion

The proposed method was found to be applicable for the investigation of active electrochemical reaction sites in limited experimental conditions. The lateral resolution of the active site imaging with the present equipment was around 1 μm when the sample was treated at 973 K. The largest factor to determine the resolution was the quenching rate. It was difficult to visualize the reaction site when YSZ was treated at 973 K due to the difficulty in quenching. In the present equipment, the sample can not be cooled directly. The improvement is necessary for the study in further detail. Also, the electrode should be prepared in a well defined structure for more quantitative analysis.

The existence of 'hot spots' could be shown for the low temperature electrode reaction. From a view point of designing a practical electrode, the inhomogeneity of the current distribution is a serious problem. The isotope imaging method can be a useful technique to investigate rather macroscopic distributions of the reaction sites.

References

[1] J. Mizusaki, K. Amano, S. Yamauchi, K. Fueki, Solid State Ionics 22 (1987) 313.
[2] M. Kleitz, L. Dessemond, T. Kloidt, Space Expansions of the Regular Oxygen Electrode Reaction on YSZ, abstract 110A p. 35 in Extended Abstracts of the 3rd Symp. on Solid Oxide Fuel Cells in Japan, Tokyo, 1994.
[3] J. Fleig, J. Maier, J. Electrochem. Soc. 144 (1997) L302.
[4] K. Kawada, A. Masuda, K. Kaimai et al., in: A.J. McEvoy, K. Nisancioglu (Eds.), Proc. 10th SOFC Workshop, IEA Programme of R, D&D on Advanced Fuel Cells, 28–31 January 1997, Les Diablerets, CH, International Energy Agency, 1997, p. 146.
[5] R.J. Chater, S. Carter, J.A. Kilner, B.C.H. Steele, Solid State Ionics 53–56 (1992) 859.
[6] H. Haneda, C. Monty, J. Am. Ceram. Soc. 72 (1989) 1153.
[7] T. Kawada, T. Horita, N. Sakai, H. Yokokawa, M. Dokiya, Solid State Ionics 79 (1995) 201.

[8] T. Kawada, T. Horita, N. Sakai, H. Yokokowa, M. Dokiya, J. Mizusaki, Proc. the 2nd Intern. Meeting of Pacific Rim Ceramic Societies (PacRim-2), 15–17 July 1996, Cairns, Australia, pp. 543–565.

[9] T. Horita, K. Yamaji, M. Ishikawa, N. Sakai, H. Yokokawa, T. Kawada, T. Kato, J. Electrochem. Soc. 145 (9) (1998) 3196.